ELSEVIER

Chemical Engineering Journal 118 (2006) 133–139

Chemical Engineering Journal

www.elsevier.com/locate/cej

H_2S catalytic oxidation on impregnated activated carbon: Experiment and modelling

Li Wang, Bin Cao, Shudong Wang, Quan Yuan *

Dalian Institute of Chemical Physics, Chinese Academy of Sciences, 457 Zhongshan Road, Dalian 116023, China

Received 19 June 2005; received in revised form 8 December 2005; accepted 19 December 2005

Abstract

A mathematic model of H_2S catalytic oxidation on impregnated activated carbon with fouling of catalyst has been developed. Kinetic studies were carried out in a fixed activated carbon bed under atmospheric pressure and low temperature (30–80 °C). The effects of flow rate, H_2S inlet concentration, temperature and relativity humidity were analyzed. Experimental results of breakthrough curves were used to obtain kinetic parameters accounted for axial dispersion, external and internal mass-transfer resistances as well as effects of S deposition on inner-face of the catalyst. The model described satisfactorily the experimental breakthrough curves and well explained the performance of oxidation. The exothermic heat of adsorption and activation energy assuming Arrhenius type of temperature dependence of the equilibrium constant was determined to be 44.6 and 29.9 kJ/mol, respectively. ε_{p0}, α and β were used to quantify the behavior of H_2S oxidation at different operating conditions. The effect of relative humidity on ε_{p0}, α and β is significant in the relative humidity range under study. The mathematic model can be considered as a reliable tool for process design and scale-up of similar system.

Keywords: Hydrogen sulfide; Catalytic oxidation; Impregnated activated carbon; Kinetic modelling

1. Introduction

Hydrogen sulfide originating from various sources such as chemical processing gases from coal, natural gas and synthesis gas can be regarded as a major air pollution, meanwhile even ppm levels of H_2S are detrimental to the catalyst. Due to stricter environmental policies of zero emission and avoidance catalyst deactivation, highly efficient removal of sulfur compounds has been claimed.

The conventional ways for H_2S removal [1] include amine aqueous solution, adsorption-clause process, liquid redox process and fixed-bed solid adsorption process which has been widely investigated at higher temperature (300–500 °C) [2]. Another method for removal H_2S is by direct oxidation at lower temperatures (lower than 100 °C) in the presence of a catalyst. Activated carbon is widely used as the support because of its developed surface area, micro porosity, high sorption capacity and easily modified surface properties [3]. Highly efficient removal (sulfur emission on ppb level) and high sulfur capacity up to 60% (g/g cat.) are obtained by catalytic oxidation on impregnated activated carbon.

Most of the prior investigations of the catalytic reaction on activated carbon are $H_2S(g) + (1/2)O_2 \rightarrow H_2O(g) + S$. Elemental sulfur formed in the oxidation is deposited on the carbon catalyst which causes the continuous change in the effectiveness factor due to the texture of the catalyst changing as a result of sulfur deposition and the gradual decrease in the number of active sites due to their physical covering by sulfur [4]. Usually it is possible to draw a parallelism between sulfur deposition on carbon catalyst like coke lay-down on catalysts used in many hydrocarbon reactions such as cracking, isomerization and hydrocracking [5]. The amount of sulfur formed on (W_s) was calculated by graphical integration from the breakthrough curves, then the reciprocal of the amount of sulfur formed on (W_s) is plotted against the reciprocal of time to processing the data [6]. However, kinetic parameters are obtained by this kind of data process, the effect of S deposition on inner-face of the catalyst resulted in the increase of mass-transfer resistance and the decrease of the number of active sites are all attribute to one parameter which would cause

* Corresponding author.
E-mail address: qyuan@dicp.ac.cn (Q. Yuan).

1385-8947/$ – see front matter © 2006 Elsevier B.V. All rights reserved.
doi:10.1016/j.cej.2005.12.021

Nomenclature

C	concentration in the bulk phase
C_m	concentration at catalyst external surface (g/m^3)
C_{out}^{cal}	calculated outlet concentration
C_{out}^{exp}	experimental outlet concentration
C_p	internal concentration in particle (g/m^3)
d_p	particle diameter (m)
D_m	film mass-transfer coefficient
D_p	pore dispersion coefficient relative to particle
D_z	axial dispersion coefficient
k_f	external mass-transfer coefficient (m/s)
K_{H_2S}	adsorption constant of H_2S
m_s	function of sulfide deposition
M	molecular weight
N_e	number of experiment runs
N_s	number of sampling
P	pressure
r	radius relative to particle
R_{H_2S}	rate of reaction
Re_p	Reynolds number relative to particle
Sc	Schmidt number
Sh_p	Sherwood number relative to particle
t	time (h)
T	temperature (K)
u	velocity (m/s)
U	flow rate
$\sum V$	special diffusion parameters
W_s	saturation sulfur capacity (g/g cat.)
z	bed length (m)

Greek letters

α	deactivation coefficient
β	sulfide deposition coefficient
ε_b	bulk porosity
ε_p	bulk porosity relative to particle
ε_{p0}	initial bulk porosity relative to particle
$\phi(m_s)$	deactivation function
φ	objective function for optimization (Eq. (17))
μ_f	dynamic viscosity (Pa s)
ρ_f	particle density

confused understanding of the performance of catalyst fouling.

In this paper, the kinetics was studied in lower relative humidity (RH: 5–60%) and at higher temperature (30–80 °C) using a mathematic model that took account of both external and internal mass-transfer resistance as well as effects of S deposition on inner-face of the catalyst. The influences of operating variables on the catalytic oxidation on impregnated activated carbon in a fixed bed were investigated. The application of the model to catalytic removal of H_2S in a fixed bed can provide a reasonable basis for analysis and scale-up of similar industrial gas purification systems.

2. Experiments

2.1. Materials

The catalysts supplied by Dalian Purit Co. were made of a commercial activated carbon whose characteristics are presented in Table 1. The catalysts were prepared by an incipient wet impregnation in which 6% Na_2CO_3 aqueous was adsorbed onto the activated carbon. The catalyst has such advantage of high efficient removal and sulfur capacity that are successfully operated in natural gas desulfurizing installation with the capacity 600,000 m^3/day.

2.2. Experimental apparatus

A schematic flow diagram of the catalytic oxidation process is shown in Fig. 1. A fixed-bed used for this study was constructed from glass tube 12.5 mm i.d. and 550 mm in length. The concentration of water in the feed was regulated by choosing a saturation temperature giving the desired water vapor pressure in a specified flow rate of the carrier gas (N_2). By adjusting the water bath temperature to deliver appropriate vapor pressure of water, and by regulating both H_2S and N_2 flow-rates, the feed compositions could be adjusted over a wide range. In each experiment, 3.5 g catalysts with particle size 1.5 mm × 1.5 mm were in use. H_2S was measure by sulfur Micro-coulomb analyzer and

Table 1
Properties of the catalyst

Parameters	Value
Total surface area (N_2, BET method) (m^2/g)	838.8
Total pore volume (ml/g)	1.216
Micro pore volume (BDB) (ml/g)	1.1033
Apparent density (bulk density, dense packing) (g/cm^3)	0.47
Real density (He displacement) (g/cm^3)	1.8

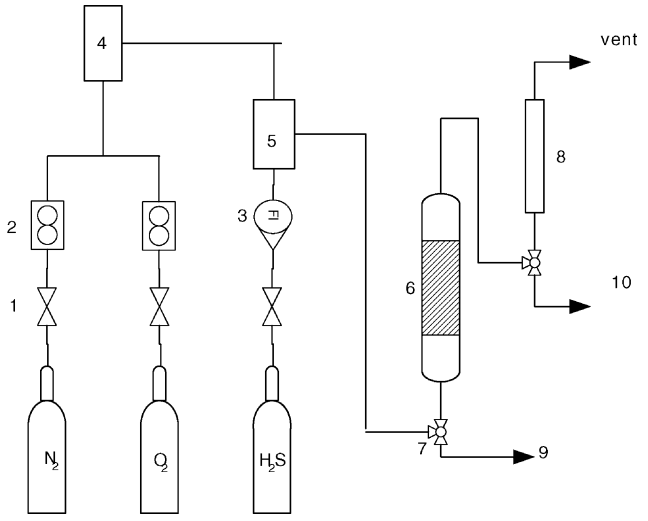

Fig. 1. Schematic diagram of experimental system. (1) Micro-valve, (2) mass flow meter, (3) rotameter, (4) humidifier, (5) mixer, (6) reactor, (7) three-way valves, (8) manometer, (9) feed analysis and (10) tail gases analysis.

Varian 3800 gas chromatograph with a pulsed flame photometric detector permitting the detection at levels as low as 0.5 ppm.

The oxidation of H_2S was studied at temperature ranging from 30 to 80 °C with H_2S content varying from 1500 to 5500 ppm. The fixed O_2/H_2S stoichiometric ratio of 2 was supplied to the catalysts. Water content was varied from relative humidity at 5–60%. A total flow of 500 ml/min was used with a GHSV of 5000 h^{-1}.

3. Mathematical model

In present study, the following assumptions were made to modelling the process:

(1) The process operates under isothermal conditions.
(2) Packed porosity is constant along the longitudinal axis of the bed.
(3) Axial dispersion plug-flow model is adopted to account for non-ideal flow in the bed.
(4) The catalyst particle is assumed to be spherical and homogeneous in size and density.
(5) Mass transport between the bulk and the solid particle is described by the external-film mass-transfer coefficient k_f. Intraparticle mass transfer is characterized by the pore-diffusion coefficient D_p.
(6) In these experiments, the ratio of O/S and H_2O/S is very large, the influence of O_2 and H_2O concentration on oxidation is negligible, so we can assume that the concentration of O_2 and H_2O remains constant along the bed.

3.1. Reactor model

The overall mass balance around the fixed bed can be expressed as

$$\frac{\partial C}{\partial t} + u\frac{\partial C}{\partial z} = D_z\frac{\partial^2 C}{\partial z^2} + \frac{3k_f}{R_p}\frac{1-\varepsilon_b}{\varepsilon_b}(C_p|_{r=R_p} - C) \quad (1)$$

The initial and Danckwerts boundary conditions at both ends of the bed are given by the following equations:

$$\text{at } t = 0, \quad C = 0 \quad (2)$$

$$\text{at } t > 0, \quad z = 0, \quad D_z\frac{\partial C}{\partial z} = u(C - C_{in}) \quad (3)$$

$$\text{at } t > 0, \quad z = L, \quad \frac{\partial C}{\partial z} = 0 \quad (4)$$

The Wakao–Funazkri correlation [7] was adopted to estimate the film mass-transfer coefficient and axial dispersion coefficient

$$Sh_p = 2 + 1.1Sc^{1/3}Re_p^{0.6}, \qquad \frac{\varepsilon_b D_z}{D_m} = 20 + 0.5Sc\,Re_p \quad (5)$$

where Sh_p and Re_p are the Sherwood and Reynolds numbers relative to particle

$$Sh_p = \frac{k_f d_p}{D_m}, \qquad Re_p = \frac{d_p U\rho_f}{\mu_f} \quad (6)$$

Sc is the Schmidt number

$$Sc = \frac{\mu_f}{\rho_f D_m} \quad (7)$$

The molecular diffusivity in multicomponent gas, D_m, was calculated by the Fuller–Schettler–Gridding method [8].

$$D_{AB} = \frac{0.00143T^{1.75}}{PM_{AB}^{1/2}[(\sum V_A)^{1/3} + (\sum V_B)^{1/3}]^2}.$$

3.2. Intraparticle mass transfer

The mass transport within a catalyst particle can be represented by the following reaction–diffusion equation:

$$\frac{\partial(\varepsilon_p C_p)}{\partial t} = \frac{1}{r^2}\frac{\partial}{\partial r}\left(r^2 D_p(r,t)\frac{\partial C_p}{\partial r}\right) - R_{H_2S} \quad (8)$$

The sulfide deposition in the particle was governed by

$$\frac{\partial m_s}{\partial t} = R_{H_2S} \quad (9)$$

The random pore model [9] was used to estimate the pore-diffusion coefficient D_p, which is calculated by the following equation:

$$D_p(r,t) = D_m\varepsilon_p^2 \quad (10)$$

where ε_p is given by

$$\varepsilon_p(r,t) = \varepsilon_{p0} - \beta m_s(r,t) \quad (11)$$

together with the initial conditions

$$\text{at } t = 0, \quad C_p = 0, \quad m_s = 0 \quad (12)$$

The mass-transfer boundary conditions on the surface of the catalyst is expressed as

$$\text{at } t > 0, \quad r = R_p, \quad D_p\frac{\partial C_p}{\partial r} = k_f(C - C_p|_{r=R_p}) \quad (13)$$

The symmetry conditions at the center of the particles is as follows:

$$r = 0, \quad \frac{\partial C_p}{\partial r} = 0. \quad (14)$$

3.3. Kinetic model

Based on the results of our experiments and other researchers [10], the expression of reaction rate is taken as:

$$R_{H_2S} = \frac{k_{H_2S}K_{H_2S}C_{H_2S}}{1 + K_{H_2S}C_{H_2S}}\phi(m_s) \quad (15)$$

where $\phi(m_s)$ is the deactivation function, it is expressed as follows:

$$\phi(m_s) = \exp(-\alpha m_s) \quad (16)$$

The method of finite volume was applied to discretize the space variables z and r of the partial differential Eqs. (1) and (8),

and the resulting ordinary differential equations were numerically integrated by Gear's method.

The values of ε_{p0}, α, β, k_{H_2S} and K_{H_2S} were determined by minimizing the difference between calculation and experimental outlet concentration of H_2S using the objective function of

$$\varphi = \sum_{i=1}^{N_e}\sum_{j=1}^{N_s}\left(\frac{C_{out,j,i}^{exp} - C_{out,j,i}^{cal}}{C_{in,i}^{exp}}\right)^2 \quad (17)$$

where N_e is the number of experiment runs and N_s is the number of sampling. The BFGS algorithm was adopted to search the optimum fitting value of the parameters.

4. Results and discussion

During these experiments, because the concentration of outlet H_2S is changing from several to thousands ppm with the time, it is appropriate to draw the outlet breakthrough curves with the logarithm coordinates.

4.1. Effects of temperature

The outlet of H_2S over the time as a function of temperature at 30, 50, 70 and 80 °C are plotted in Figs. 2–7. The oxidation of H_2S is an exothermic reaction and highly thermodynamically favorable to product side. This reaction is sensitive to the temperature and input H_2S concentration. With lower inlet H_2S, the amount S deposited on the catalyst is less which resulted in lower deactivation rate. For the faster initial reaction rate is, the more sulfur deposited on the support which causes the lower mass-transfer flux from the bulk to the particle and the more decrease of active sites.

4.2. Effects of relative humidity

The effect of the relative humidity on the kinetic oxidation was studied. The results from those runs conducted at 50 °C are plotted in Figs. 6–8. The results indicate that H_2S conversion is affected to a significant extent by increasing the water vapor up to 60% in the feed. With the increase of relative humidity in the feed, the creation of water films can be significantly enhanced. The presence of a water film enables the dissociation of H_2S molecules to hydrogen sulfide ions HS^-, which are then oxidized. This beneficial effect of relative humidity was also observed in literature [11].

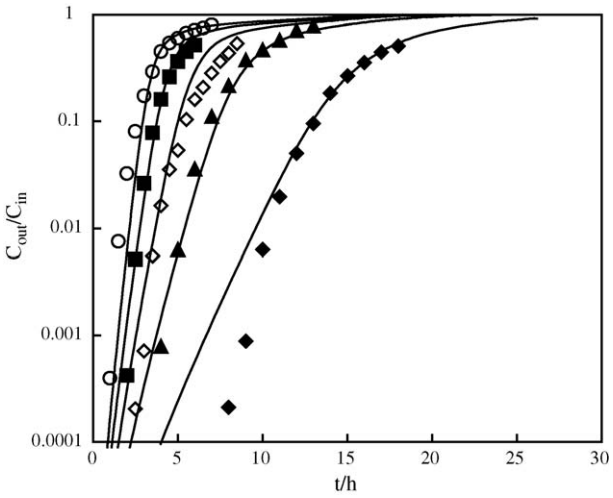

Fig. 3. Experiment (dots) and model (line) outlet concentration of H_2S for different inlet concentration at $T = 50$ °C and RH = 20%. C_{in}: (♦) 1518 ppm, (▲) 2569 ppm, (◊) 3568 ppm, (■) 4496 ppm and (◯) 5477 ppm.

4.3. Effects of space velocity

The flow rate and, thus, the linear velocity of the fluid phase affects the thickness of the boundary layer surrounding the particles and the external mass-transfer coefficient that is a function of the latter. The effect of the flow rate on the oxidation process

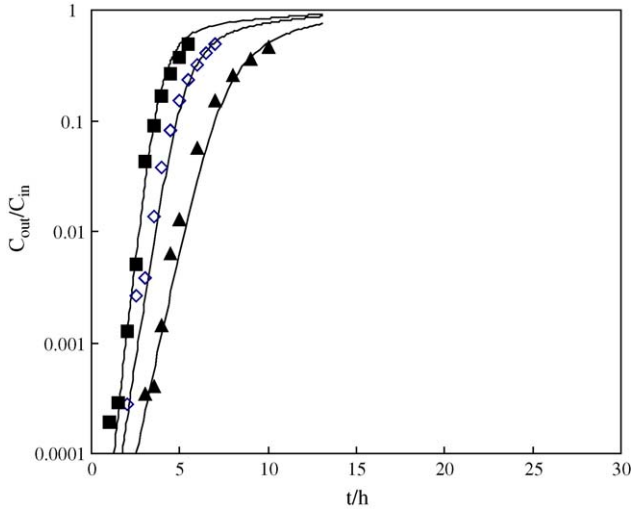

Fig. 2. Experiment (dots) and model (line) outlet concentration of H_2S for different inlet concentration at $T = 30$ °C and RH = 20%. C_{in}: (▲) 2540 ppm, (◊) 3520 ppm and (■) 4509 ppm.

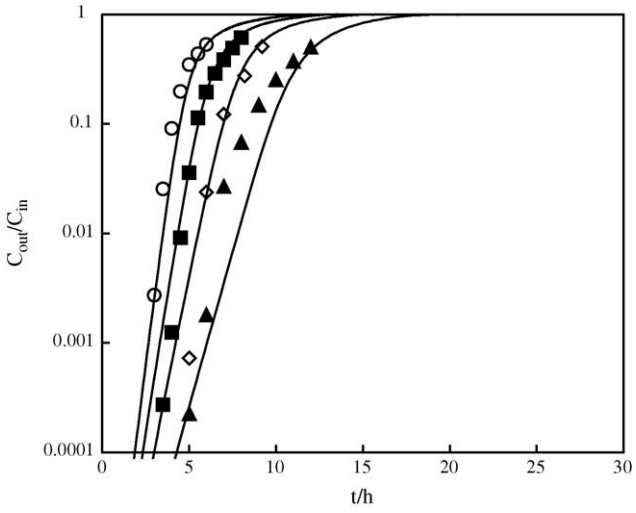

Fig. 4. Experiment (dots) and model (line) outlet concentrations of H_2S for different inlet concentration at $T = 70$ °C and RH = 20%. C_{in}: (▲) 2490 ppm, (◊) 3551 ppm, (■) 4462 ppm and (◯) 5448 ppm.

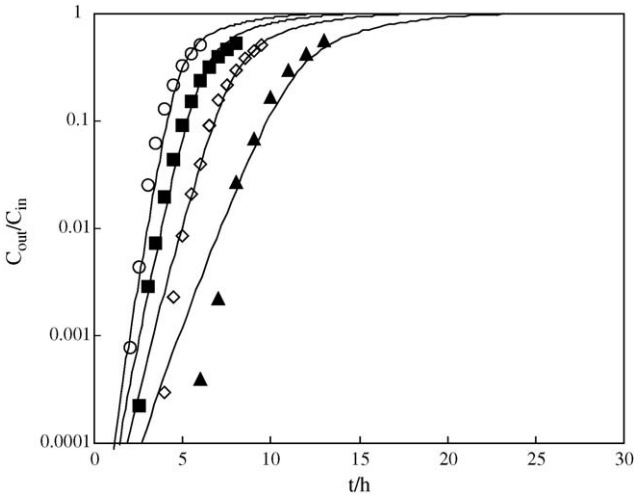

Fig. 5. Experiment (dots) and model (line) outlet concentration of H_2S for different inlet concentration at $T = 80\,^{\circ}C$ and RH = 20%. C_{in}: (▲) 2448 ppm, (◊) 3467 ppm, (■) 4434 ppm and (◯) 5537 ppm.

is characterized by the external-film mass-transfer coefficient. Within the experimental range, the external diffusion was also a mass-transfer control mechanism. The value of k_f is suitable at low Reynolds numbers.

Within the experimental range, the H_2S conversion increases with a decrease of space velocity. At lower space velocity, the residence times of H_2S and O_2 are longer and there is a great probability of collisions on the surface resulting in an increase in H_2S conversion.

As seen from Figs. 2–9, the experimental data were not in accordance well with the model data in the range of lower concentration and the initial stage of breakthrough, so there may be caused by measure error during analysis, which also could be enlarged with logarithm coordinates.

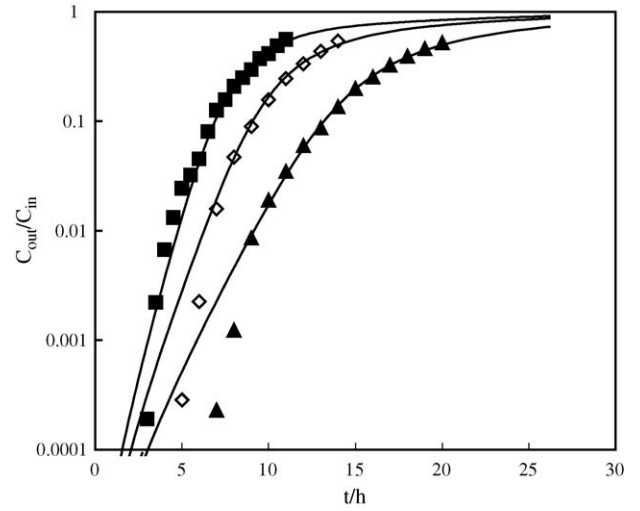

Fig. 6. Experiment (dots) and model (line) outlet concentration of H_2S for different relative humidity at $T = 50\,^{\circ}C$ and RH = 60%. C_{in}: (▲) 2532 ppm, (◊) 3594 ppm and (■) 4574 ppm.

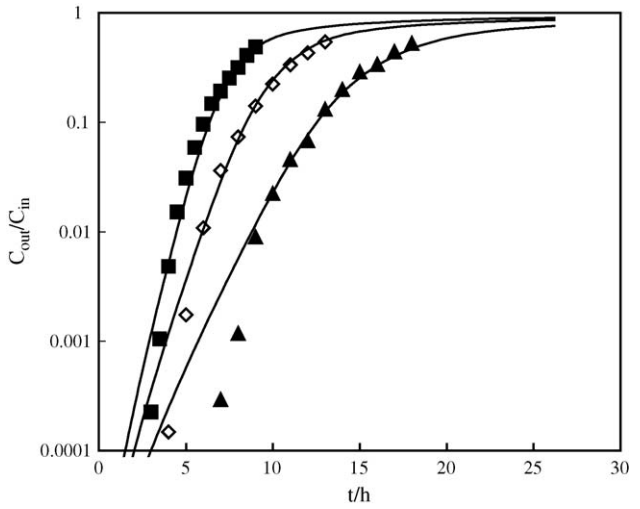

Fig. 7. Experiment (dots) and model (line) outlet concentration of H_2S for different relative humidity at $T = 50\,^{\circ}C$ and RH = 40%. C_{in}: (▲) 2568 ppm, (◊) 3581 ppm and (■) 4535 ppm.

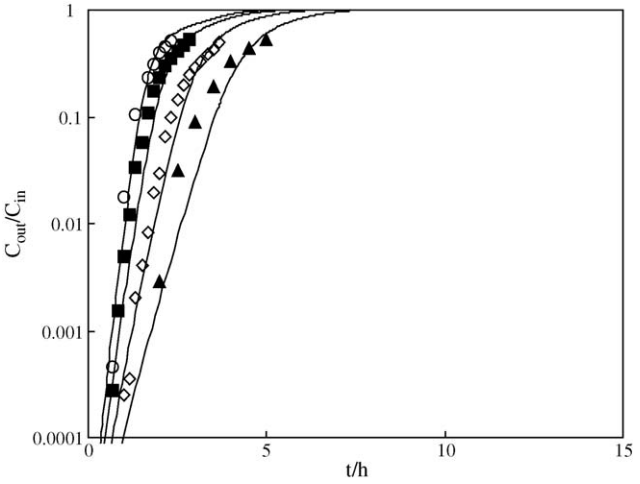

Fig. 8. Experiment (dots) and model (line) outlet concentration of H_2S for different inlet concentration at $T = 50\,^{\circ}C$ and RH = 5%. C_{in}: (▲) 2535 ppm, (◊) 3453 ppm, (■) 4552 ppm and (◯) 5529 ppm.

4.4. Model parameters analysis

The mathematical model describing the kinetics of the oxidation process was used to fit the experimental breakthrough curves in order to determine the parameters by minimization of the objective function as previously described. The best fitting values of the parameters for both are shown in Tables 2 and 3.

Table 2
Optimum model parameters at different operating temperature

T (°C)	ε_{p0}	α ($\times 10^4$)	β ($\times 10^5$)	k_{H_2S}	K_{H_2S}
30	0.33	5.78	3.78	5.41	200.0
50	0.34	6.04	3.95	5.97	80.44
70	0.38	6.00	4.00	20.00	50.00
80	0.38	6.06	4.00	25.13	11.54

RH = 20%, GHSV = 4980 h^{-1}.

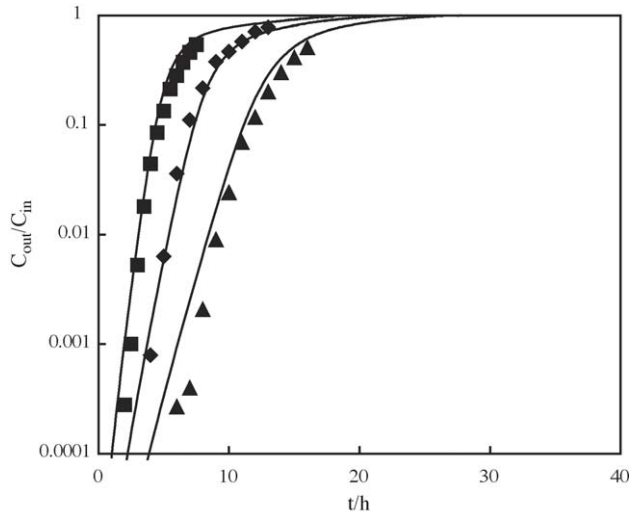

Fig. 9. Experiment (dots) and model (line) outlet concentration of H_2S for different inlet concentration at $T = 50\,^{\circ}C$ and RH = 20%, $C_{in} \approx 2500$ ppm. GHSV: (▲) 3623 h^{-1}, (◊) 4980 h^{-1} and (■) 7229 h^{-1}.

Table 3
Optimum model parameters at different relative humidity

RH (%)	ε_{p0}	α ($\times 10^4$)	β ($\times 10^5$)	k_{H_2S}	K_{H_2S}
5	0.35	10.51	8.87	4.40	79.41
20	0.34	6.04	3.95	5.97	80.44
40	0.28	3.62	1.51	6.99	80.07
60	0.27	3.18	1.56	7.54	80.05

$T = 50\,^{\circ}C$, GHSV = 4980 h^{-1}.

Arrhenius equation was used to get the parameters of adsorption heat and activation energy (shown in Figs. 10 and 11). The heat of adsorption 44.6 kJ/mol was found to be positive as it is an exothermic process; therefore, K_{H_2S} decreased from 200 to 11.54 with the increase of temperature from 30 to 80 °C. The activation energy of H_2S oxidation was 29.9 kJ/mol and with an increase in the operating temperature yielded higher values of reaction rate constant.

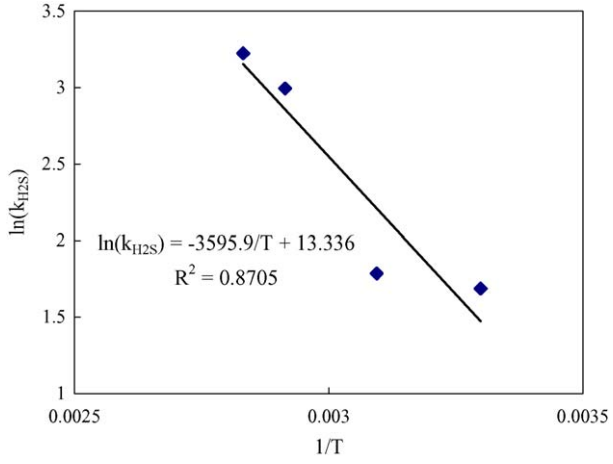

Fig. 10. $\ln(k_{H_2S})$ as a function of $1/T$.

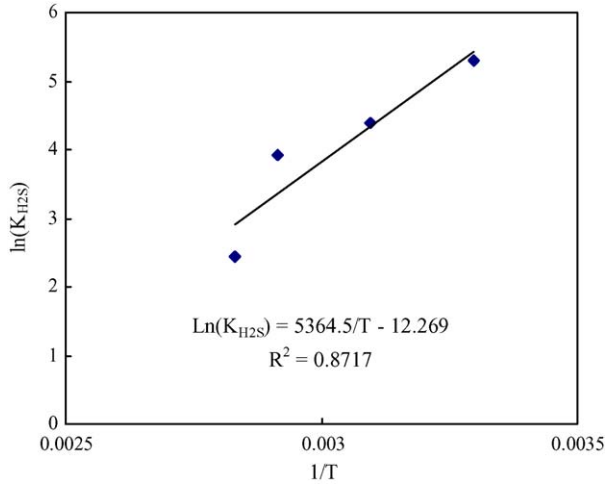

Fig. 11. $\ln(K_{H_2S})$ as a function of $1/T$.

With the increase of relative humidity in the feed, the creation of water films can be significantly enhanced which cause the decrease of ε_{p0}. The presence of a water film enables the dissociation of H_2S molecules to hydrogen sulfide ions HS^-, which are then oxidized to sulfur polymers having chain or ring-like shapes soluble in water film. The water plays an important role in H_2S oxidation, however the adsorption constant K_{H_2S} is not influenced by the relative humidity. This means probably that the competitive effective of the water in the adsorption is counterbalanced by the increase of dissolving O_2 and H_2S in the water film [10]. The enhancement in oxidation H_2S due to the presence of water was also observed by other authors [12]. The presence of water slows down the deactivation process by promoting deposition and adsorption of sulfur on different carbon sites and/or by mechanically removing sulfur from active sites which all results in the decrease of α and β. The presence of water-dissolved sulfur species was also observed in the regeneration of exhausted carbon feasible [13].

5. Conclusions

A mathematic model about catalytic oxidation of H_2S on activated carbon accounting for external-film and pore-diffusion mass-transfer mechanism, axial dispersion was used to fit the experimental breakthrough curves. The model reproduced adequately the experimental results and best fitting parameters were attained.

Adsorption heat and activation energy obtained by Arrhenius equation were 44.6 and 29.9 kJ/mol, respectively. The parameters ε_{p0}, α and β with respect of the catalyst were used to quantify the performance of the process at different operating conditions. The temperature favors the effectiveness of the reaction rate constant, although the adsorption constant decrease in these conditions. The efficiency increases with relative humidity as the decrease of parameters ε_{p0}, α and β. It was also observed that the effect of relative humidity on ε_{p0}, α and β is much more significant than temperature in the study range.

References

[1] R. Wang, Investigation a new liquid redox method for removal H_2S and sulfur recovery with heteropoly compound, Sep. Purif. Technol. 31 (2003) 111–121.

[2] E. Sasaoka, Characterization of reaction between zinc oxide and hydrogen sulfide, Energy Fuels 8 (1994) 1100–1105.

[3] R.C. Bansal, J.B. Donnet, F. Stoeckli, Activated Carbon, Dekker, New York, 1988.

[4] R. Dreeramamurthy, P.G. Menon, Oxidiation of H_2S on activated carbon catalyst, J. Catal. 37 (1975) 287–296.

[5] A. Voorhies, Carbon formation in catalytic cracking, Ind. Eng. Chem. 37 (1945) 318–322.

[6] A.N. Kaliva, J.W. Smith, Oxidization of low concentration of hydrogen sulfide by air on a fixed activated carbon, Can. J. Chem. Eng. 61 (April) (1983) 208–212.

[7] N. Wakao, T. Funazkrib, Effect of fluid dispersion coefficients on particle-to-fluid mass transfer coefficients in packed beds, Chem. Eng. Sci. 33 (1978) 1375–1384.

[8] E.N. Fuller, P.D. Schettler, J.C. Giddings, A new method for prediction of binary gas-phase diffusion coefficients, Ind. Eng. Chem. 58 (May) (1966) 18–27.

[9] G.F. Froment, K.B. Bischoff, Chemical Reactor Analysis and Reactor", John Wiley & Sons, New York, 1990.

[10] X.Y. Tan, The Process to Remove H_2S on Impregnated Activated Carbon[D], Dalian Institute of Chemical Physics, Chinese Academy of Sciences, 1999.

[11] A. Primavera, A. Trovarelli, P. Andreussi, The effect of water in the low-temperature catalytic oxidization of hydrogen sulfide to sulfur over activated carbon, Appl. Catal. A: Gen. 173 (1998) 185–192.

[12] A. Bagreev, T.J. Bandosz, H_2S adsorption/oxidation on unmodified activated carbons: importance of prehumidification, Carbon 39 (2001) 2303–2311.

[13] T.J. Bandosz, Q. Le, Evaluation surface properties of exhausted carbons used as H_2S adsorbents in sewage treatment palnts, Carbon 36 (1998) 39–44.